Theoretical Study on the Bromomethane−Water 1:2 Complexes

Weizhou Wang,*,† Anmin Tian,‡ and Ning-Bew Wong§

Department of Chemistry, Huazhong University of Science and Technology, Wuhan, Hubei 430074, China, Faculty of Chemistry, Sichuan University, Chengdu, Sichuan 610014, China, and Department of Biology and Chemistry, City University of Hong Kong, Kowloon, Hong Kong

Received: May 16, 2005; In Final Form: July 12, 2005

Bromomethane−water 1:2 complexes have been theoretically studied to reveal the role of hydrogen bond and halogen bond in the formation of different aggregations. Four stable structures exist on the potential energy surface of the $CH_3Br(H_2O)_2$ complex. The bromine atom acts mainly as proton acceptor in the four studied structures. It is also capable of participating in the formation of the halogen bond. The properties and characteristics of the hydrogen bond and the halogen bond are investigated employing several different quantum chemical analysis methods. Cooperative effects for the pure hydrogen bonds or the mixed hydrogen bonds with halogen bonds and the possibility of describing cooperative effects in terms of the topological analysis of the electronic density or the charge-transfer stabilization energy are discussed in detail. An atoms-in-molecules study of the hydrogen bond or the halogen bond in the bromomethane−water 1:2 complexes suggests that the electronic density topology of the hydrogen bond or the halogen bond is insensitive to the cooperative effect. The charge-transfer stabilization energy is proportional to the cooperative effect, which indicates the donor−acceptor electron density transfer to be mainly responsible for the trimer nonadditive effect.

Introduction

The number of individual crystal structures in which weak interactions have been reported to be important has grown rapidly in recent years.[1−3] Therefore, understanding the nature of these intermolecular interactions is a necessary step toward a full rationalization of the packing and also a key preliminary step in the design of new crystals. Considering that crystal packing results as the sum of many different contributions of directional and nondirectional intermolecular interactions, it is important that different types of interactions be considered jointly in structure analysis. Although researches have traditionally focused on the more well-known hydrogen bonded interactions,[3−6] a growing body of experimental and theoretical evidence confirms that interactions such as −X···Y− (X = Cl, Br, or I; Y = N, O, S, or π) and even interactions such as −X···Y− (X = Cl, Br, or I; Y = Cl, Br, or I) may also play distinctive roles in crystal formation;[7−30] as we know, such interactions are the so-called halogen bonding. Very recently, Auffinger et al. exploited the halogen-bonded interactions in the crystal structures of halogenated biomolecules.[31] Their survey of protein and nucleic acid structures reveals similar halogen bonds as potentially stabilizing inter- and intramolecular interactions that can affect ligand binding and molecular folding.

The halogen atoms act as donors in the halogen bonds, on one hand, and they are also capable of participating in hydrogen bonds and are good hydrogen acceptors on the other hand.[3] Also very recently, by X-ray single-crystal diffraction analysis, Zhu et al. reported the example that coexisting intermolecular hydrogen bonding and halogen bonding share one same bromine atom in the crystal structure of compound *trans*-5,10-bis(1-bromodifluoroacetyl-1-(ethoxycarbonyl)methylidene)thianthrene.[32] How about the hydrogen bonding pattern and the halogen bonding pattern around the halogen atoms? Can the halogen atom act in a dual role in other systems? What about the cooperative nature of hydrogen bonds and halogen bonds around the halogen atoms? These are questions to which the following calculations should give a clue. In the present paper, we report the result of a quantum chemical study of the stability, structure, hydrogen bonding or halogen bonding pattern, topological analysis of the electronic density, and charge transfer analysis of different orbitals of bromomethane−water 1:2 complexes. It must be pointed out that, in biological systems, the halogen bond is mainly of the C−X···O−Y type, where C−X is a carbon-bonded chlorine, bromine, or iodine, and O−Y is a carbonyl, hydroxyl, charged carboxylate, or phosphate group,[31] and on the other hand the halogen bond is hard to form in other bromomethane−water 1:*n* complexes, where $n \neq 2$;[33] therefore, bromomethane−water 1:2 complexes are very good models for biological systems.

Computational Details

The Second-order Møller−Plesset theory (MP2)[34] has been shown to be effective and accurate in determining the equilibrium structure and binding energy for many hydrogen bonded and other weakly bound complexes.[35] The Pople's moderate 6-31G(d,p)[36] basis set has been proved to produce reliable data on hydrogen bonding previously.[37] The basis set applied here is Dunning's correlation consisted basis sets aug-cc-pVDZ and aug-cc-pVTZ.[38] In the present study, an especially thorough search for all the low-lying energy structures has been done at the MP2(full)/aug-cc-pVDZ level. No symmetries were constrained in optimizations. Finally, we obtained four low-lying energy conformers: **M1**, **M2**, **M3**, and **M4** (see Figure 1). The four conformers are all confirmed as true minima on the potential energy surface of bromomethane−water 1:2 complex

* To whom correspondence should be addressed. E-mail: wzwanglab@yahoo.com.
† Huazhong University of Science and Technology.
‡ Sichuan University.
§ City University of Hong Kong.

10.1021/jp052557c CCC: $30.25
Published on Web 08/16/2005

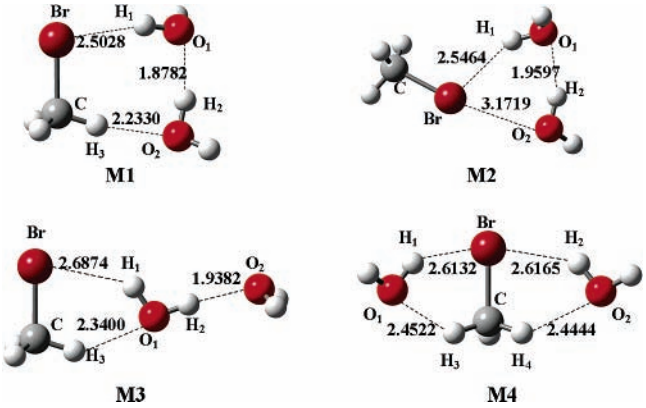

Figure 1. MP2(full)/aug-cc-pVDZ optimized low-energy structures (distances in Å) of complex $CH_3Br(H_2O)_2$. The dashed lines indicate hydrogen bonds or halogen bonds.

by the presence of only real frequencies after the corresponding harmonic vibrational analysis at the same theory level. Other properties were all calculated using the aug-cc-pVTZ basis set at the MP2(full)/aug-cc-pVDZ optimized geometries. The basis set superposition error (BSSE) was eliminated by the standard counterpoise (CP) correction method of Boys and Bernard.[39]

For a complex ABC made up of three interacting subsystems A, B, and C, the total interaction energy ΔE_{Tot} can be evaluated as the difference in energy between the complex and the three isolated monomers, A, B, and C,

$$\Delta E_{\mathrm{Tot}} = E_{\mathrm{ABC}}^{\mathrm{ABC}} - (E_{\mathrm{A}}^{\mathrm{A}} + E_{\mathrm{B}}^{\mathrm{B}} + E_{\mathrm{C}}^{\mathrm{C}}) \quad (1)$$

defining $E_{\mathrm{X}}^{\mathrm{Y}}$ as the energy of system X with basis set Y. This energy is then corrected via the counterpoise method by calculating the energy of each monomer using the same, trimer, basis set,

$$\Delta E_{\mathrm{Tot}}^{\mathrm{CP}} = E_{\mathrm{ABC}}^{\mathrm{ABC}} - (E_{\mathrm{A}}^{\mathrm{ABC}} + E_{\mathrm{B}}^{\mathrm{ABC}} + E_{\mathrm{C}}^{\mathrm{ABC}}) \quad (2)$$

The total two-body interaction energy ΔE_2^{CP} in the trimer is expressed as the sum of the difference between the energy of a given interacting pair and the energy of the corresponding isolated monomers, keeping all geometries frozen in the trimer structure

$$\Delta E_2^{\mathrm{CP}} = E_{\mathrm{AB}}^{\mathrm{ABC}} + E_{\mathrm{BC}}^{\mathrm{ABC}} + E_{\mathrm{AC}}^{\mathrm{ABC}} - 2(E_{\mathrm{A}}^{\mathrm{ABC}} + E_{\mathrm{B}}^{\mathrm{ABC}} + E_{\mathrm{C}}^{\mathrm{ABC}}) \quad (3)$$

,

The three-body nonadditive interaction energy or cooperativity is obtained from the difference between the total interaction energy and the two-body interaction energy,

$$\Delta E_3^{\mathrm{CP}} = \Delta E_{\mathrm{Tot}}^{\mathrm{CP}} - \Delta E_2^{\mathrm{CP}}$$

$$= E_{\mathrm{ABC}}^{\mathrm{ABC}} - E_{\mathrm{AB}}^{\mathrm{ABC}} - E_{\mathrm{BC}}^{\mathrm{ABC}} - E_{\mathrm{AC}}^{\mathrm{ABC}} + E_{\mathrm{A}}^{\mathrm{ABC}} + E_{\mathrm{B}}^{\mathrm{ABC}} + E_{\mathrm{C}}^{\mathrm{ABC}} \quad (4)$$

The bonding characteristics of the different complexes were analyzed by using the "atoms in molecules" (AIM) theory of Bader,[40] which is based on a topological analysis of the electron charge density and its Laplacian. The AIM theory has proved itself a valuable tool to conceptually define what is an atom, and above all what is a bond in a quantum calculation of a molecular structure. The analysis went further with those obtained by means of the natural bond obital (NBO) theory of Weinhold and co-workers.[41] The NBO analysis will allow us to quantitatively evaluate the charge transfer (CT) involving the formation of hydrogen bond or halogen bond.

All ab initio calculations were carried out with the Gaussian 03 suite of programs.[42] AIM analysis was performed with the AIM2000 software package, using the MP2(full)/aug-cc-pVTZ wave functions as input.[43] NBO analysis used the MP2-optimized structures, the Hartree−Fock (HF) densities, and the built-in subroutines of the Gaussian 03 program.

TABLE 1: Selected Geometrical Parameters (Å and deg) and Frequencies (cm^{-1}) for Bromomethane, Water, and Four Low-Energy Structures M1, M2, M3, and M4 at the MP2(full)/aug-cc-pVDZ Level[a]

			complexes			
parameters	CH_3Br	H_2O	**M1**	**M2**	**M3**	**M4**
O_1-H_1		0.9652	0.9722	0.9715	0.9670	0.9685
freq (O_1-H_1)		3808.1	3719.4	3733.6	3697.8	3767.8
O_2-H_2		0.9652	0.9764	0.9737		0.9686
freq (O_2-H_2)		3808.1	3628.2	3679.5		3765.6
C−Br	1.9440		1.9545	1.9453	1.9501	1.9569
freq (C−Br)	634.7		617.4	633.2	626.6	616.2
$C-H_3$	1.0946		1.0951		**1.0944**	**1.0942**
freq ($C-H_3$)	3240.4		3245.9		**3247.3**	**3253.5**
$C-H_4$	1.0946					**1.0942**
freq ($C-H_4$)	3240.4					**3253.5**
$\angle O_1-H_1-Br$			163.6	152.2	136.4	140.5
$\angle C-H_3-O_1$			168.6		138.9	134.3
$\angle C-H_4-O_2$						133.7

[a] Atomic numbering is defined in Figure 1.

TABLE 2: Calculated Total Energies (au), Relative Energies (kcal/mol), and Interaction Energies (kcal/mol) of Four Minimum-Energy Structures M1, M2, M3, and M4 at the MP2(full)/aug-cc-pVTZ and HF/aug-cc-pVTZ (in Bold) Levels of Theory

structures	E_{Tot}	E_{Rel}	ΔE_{Tot}	$\Delta E_{\mathrm{Tot}}^{\mathrm{CP}}$	ΔE_2^{CP}	ΔE_3^{CP}
M1	−2765.2951956	0.00	14.72	10.84	9.57	1.27
	−2764.2217082	**0.00**	**5.95**	**6.42**	**5.11**	**1.31**
M2	−2765.2896706	3.47	11.26	7.83	7.20	0.63
	−2764.2166069	**3.20**	**2.74**	**3.08**	**2.43**	**0.65**
M3	−2765.2894773	3.59	11.14	8.29	8.29	0.00
	−2764.2196945	**1.26**	**4.68**	**4.87**	**4.86**	**0.01**
M4	−2765.2890564	3.85	10.87	6.78	6.84	−0.06
	−2764.2158514	**3.68**	**2.27**	**2.39**	**2.40**	**−0.01**

Results and Discussion

Geometrical Parameters, Interaction Energies, and Vibrational Frequencies. Some selected geometrical parameters, vibrational frequencies, and energies of four minimum-energy structures **M1**, **M2**, **M3**, and **M4** are given in Tables 1 and 2.

Table 1 shows that there is an elongation of the O_1-H_1, O_2-H_2, C−Br, or $C-H_3$ bond upon complex formation except for the $C-H_3$ and $C-H_4$ bonds in structures **M3** and **M4**, for which an increase of 0.0005−0.0112 Å is observed. The O_1-H_1 and O_2-H_2 bonds in structure **M1** are stretched by large amounts (0.0070 and 0.0112 Å). The $C-H_3$ bond in structure **M1** is stretched by only a small amount (0.0005 Å). The $C-H_3$ and $C-H_4$ bonds in structures **M3** and **M4** are all shortened upon complex formation. The $C-H_3$ bond in structure **M3** is shortened by 0.0002 Å. The $C-H_3$ and $C-H_4$ bonds in structure **M4** both are shortened by 0.0004 Å. The corresponding harmonic vibational frequencies are also shown in Table 1. The frequency analysis reveals the red-shifting character of the C−Br···O, O−H···O, and O−H···Br interactions and blue-shifting character of the C−H···O interactions. In agreement with the computed C−Br or O−H bond elongation, the C−Br

Figure 2. MP2(full)/aug-cc-pVDZ electrostatic potential surfaces of bromomethane. The blue surface represents the positive part of the electrostatic potential, and the red surface is the negative part.

or O−H stretching frequencies are lower by 1.5−18.5 or 40.3−179.9 cm^{-1} in the complexes than the corresponding frequencies in the monomers. The individual red shift can be correlated directly to the magnitude of O−H or C−Br bond elongation. Similarly, the blue shift of the C−H stretching frequency is proportional to the magnitude of the C−H bond contraction, which is consistent with the recently calculated results of the blue-shifting hydrogen bond.[44] Note that there are two exceptions. One is the O_1-H_1 bond in **M3**. The red shift of its stretching frequency cannot be correlated directly to the magnitude of O_1-H_1 bond elongation. The other is the $C-H_3$ bond in structure **M1**. As is listed in Table 1, the $C-H_3$ bond elongates upon **M1** formation, while its stretching frequency increases. This is because the O_1-H_1 or $C-H_3$ stretching vibration mode is a combination or mixture of several vibration modes. It must be pointed out that all these vibrational motions are anharmonic, and this may cast doubt on the "harmonic" results, but information from the study of the blue-shifting hydrogen bond indicates the promising adequacy of the harmonic model.[45]

According to the above analyses, we sketched the hydrogen bonding and halogen bonding patterns in Figure 1. It is very noticeable that the bromine atom in **M2** acts as an electron acceptor in the halogen bond and an electron donor in the hydrogen bond. The electrophilic portion of the neighboring H_2O molecule interacts with bromine in a "side-on" manner, nearly normal to the C−Br bond, whereas the nucleophilic region of the other H_2O molecule interacts nearly "head-on", along the C−Br axis at the Br end. This can in fact be explained from an analysis of the surface electrostatic potential. The electrostatic potential map of CH_3Br shows the anticipated negative region around the bromine and the positive region at the outermost ends of the C−Br axis (see Figure 2). In structure **M4**, the Br atom forms a bifurcated hydrogen bond with two C−H groups.

It can be seen from Table 2 that the calculated CP-uncorrected interaction energies increase in the order **M4** < **M3** < **M2** < **M1** at the MP2(full)/aug-cc-pVTZ level of theory, which is in agreement with the total energies order **M1** < **M2** < **M3** < **M4**. However, the CP-corrected interaction energies order of **M2** and **M3** is contrary to the CP-uncorrected interaction energies order of **M2** and **M3**. This is understandable since their energies, either total energies or interaction energies, are almost one and the same. The total two- and three-body interaction energies for the four studied $CH_3Br(H_2O)_2$ complexes are collected in Table 2 as well. Structure **M1** has the largest total interaction energy and the largest two- and three-body interaction energies. The three-body interaction energy of structure **M2** is equal to 0.63 kcal/mol, which is about half of the cooperativity in structure **M1**. It is worth mentioning that the three-body interaction energy is equal to zero in structure **M3**. In contrast to structures **M1**, **M2**, and **M3**, the Br atom in structure **M4** acts as a double proton acceptor. The three-body term and the resulting cooperativity then become negative (anticooperativity). Table 2 also listed the total energies and interaction energies

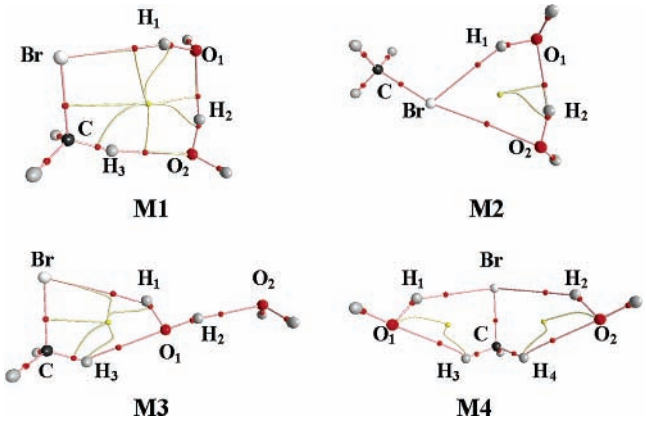

Figure 3. The molecular graphs of four low-energy structures of complex $CH_3Br(H_2O)_2$. Small red dots represent bond critical points and small yellow dots indicate ring critical points.

of the four studied structures calculated at the HF/aug-cc-pVTZ level of theory. Obviously, the HF calculations underestimate the interaction energies of the four studied systems since the HF calculations cannot evaluate the attractive dispersion interaction. A large part of the attractive interactions in these systems is covered by the HF calculations, which indicates that dispersion and electrostatics are both responsible for the attraction in these systems. Interestingly, the HF calculations yield three-body interaction energies rather close to much more accurate MP2 calculations, obviously due to the error cancellation at the HF level.

AIM Analysis. The rigorous AIM theory has been successfully applied in characterizing hydrogen bonds of different strengths in a wide variety of molecular complexes.[40,46,47] Popelier proposed a set of criteria for the existence of H-bonding within the AIM formalism.[46,47] The most prominent evidence of hydrogen bonding is the existence of a bond path between the donor hydrogen nucleus and the acceptor, containing a interatomic surface (IAS) and a bond critical point (BCP) at which the electron density (ρ_b) ranges from 0.002 to 0.035 au and the Laplacian of the electron density ($\nabla^2\rho_b$) ranges from 0.024 to 0.139 au. In our previous study,[29] we found that the three criteria for a hydrogen bond are all echoed in a halogen bond. In the present study, the properties of the BCPs of the hydrogen bonds and the halogen bonds have been examined for both the trimer and the related dimer.

Figure 3 clearly demonstrates the existence of a BCP for each noncovalent bond. The expected bond paths associated with the noncovalent bond BCPs can also be visualized in Figure 3. The electron density (ρ_b) of the bond critical point is listed in Table 3 for the hydrogen bond or the halogen bond. The values for the noncovalent bonds do fall within the proposed range of 0.002−0.035 au. It has been shown that ρ_b is related to the bond order and thus to the bond strength. As a result, the value of ρ_b is much lower for the (C)H···O bond or the (C)Br···O bond compared to the (O)H···O bond. The two negative eigenvalues of the Hessian matrix of electron density (λ_1 and λ_2) measure the degree of contraction of ρ_b perpendicular to the bond toward the critical point, whereas the positive eigenvalue (λ_3) measures the degree of contraction parallel to the bond and from the BCP toward each of the neighboring nuclei. The Laplacian $\nabla^2\rho_b$ is simply the sum of the eigenvalues λ_1, λ_2, and λ_3. It has been observed that for closed-shell interactions (ionic bonds, hydrogen bonds, and van der Waals interactions) $\nabla^2\rho_b$ is positive. According to Table 3, the noncovalent bonds are also typical closed-shell interactions, the positive values for $\nabla^2\rho_b$ lying in

TABLE 3: Density (ρ), Density Laplacian ($\nabla^2\rho$), Eigenvalues of the Hessian Matrix (λ_1, λ_2, λ_3), and Ellipticity (ϵ) at Bond Critical Points between Hydrogen (or Halogen) Bond Acceptors and Hydrogen (or Halogen) Bond Donors at the MP2(full)/aug-cc-pVTZ Level of Theory[a,b]All Units Are Atomic Units[a]

interaction	ρ_b	$\nabla^2\rho_b$	λ_1	λ_2	λ_3	ϵ
M1						
$H_1\cdots Br$	0.0164	0.0437	−0.0175	−0.0169	0.0754	0.0341
	0.0162	**0.0418**	**−0.0172**	**−0.0167**	**0.0758**	**0.0334**
$H_2\cdots O_1$	0.0294	0.0895	−0.0459	−0.0449	0.1804	0.0237
	0.0292	**0.0917**	**−0.0456**	**−0.0446**	**0.1819**	**0.0222**
$H_3\cdots O_2$	0.0137	0.0528	−0.0157	−0.0149	0.0834	0.0520
	0.0136	**0.0536**	**−0.0156**	**−0.0149**	**0.0841**	**0.0506**
M2						
$H_1\cdots Br$	0.0148	0.0396	−0.0150	−0.0148	0.0694	0.0134
	0.0146	**0.0403**	**−0.0147**	**−0.0145**	**0.0696**	**0.0153**
$H_2\cdots O_1$	0.0246	0.0824	−0.0355	−0.0338	0.1517	0.0515
	0.0245	**0.0833**	**−0.0354**	**−0.0336**	**0.1523**	**0.0509**
$Br\cdots O_2$	0.0088	0.0335	−0.0059	−0.0055	0.0449	0.0707
	0.0087	**0.0335**	**−0.0058**	**−0.0054**	**0.0447**	**0.0691**
M3						
$H_1\cdots Br$	0.0109	0.0336	−0.0096	−0.0092	0.0524	0.0401
	0.0109	**0.0333**	**−0.0096**	**−0.0093**	**0.0522**	**0.0371**
$H_3\cdots O_1$	0.0105	0.0459	−0.0100	−0.0090	0.0649	0.1115
	0.0103	**0.0457**	**−0.0098**	**−0.0088**	**0.0644**	**0.1160**
$H_2\cdots O_2$	0.0250	0.0823	−0.0376	−0.0366	0.1566	0.0275
	0.0250	**0.0824**	**−0.0376**	**−0.0366**	**0.1566**	**0.0277**
M4						
$H_1\cdots Br$	0.0126	0.0372	−0.0118	−0.0116	0.0606	0.0116
	0.0127	**0.0372**	**−0.0119**	**−0.0117**	**0.0609**	**0.0100**
$H_2\cdots Br$	0.0125	0.0372	−0.0117	−0.0115	0.0603	0.0127
	0.0126	**0.0372**	**−0.0117**	**−0.0116**	**0.0605**	**0.0102**
$H_3\cdots O_1$	0.0082	0.0364	−0.0072	−0.0057	0.0493	0.2643
	0.0081	**0.0363**	**−0.0072**	**−0.0058**	**0.0493**	**0.2504**
$H_4\cdots O_2$	0.0084	0.0370	−0.0074	−0.0060	0.0505	0.2351
	0.0083	**0.0370**	**−0.0074**	**−0.0061**	**0.0505**	**0.2302**

[a] All units are atomic units. [b] Numbers in bold are those of the corresponding dimers.

the proposed range of 0.024−0.139 au. The ellipticity ϵ is defined as $\lambda_1/\lambda_2 - 1$ and measures the extent to which charge is preferentially accumulated. The ellipticity provides a measure for not only the π character of a bond but also its structural stability. Substantial bond ellipticities reflect structural instability; that is, the bond can easily be ruptured. In Table 3 we see that ϵ((C)H···O) or ϵ((C)Br···O) is much larger than ϵ((O)H···O), confirming that the former bond is weaker, which is consistent with the case of interaction energy.

Density, density Laplacian, eigenvalues of the Hessian matrix, and ellipticity at the BCPs of the hydrogen bonds or the halogen bonds in the corresponding dimers are also presented in Table 3. The most striking phenomenon is that the density of BCPs in each trimer is almost the same as that in the corresponding dimer. The other properties such as the Laplacian, eigenvalues of the Hessian matrix, and the ellipticity are also very similar for the trimer and dimer (Table 3). The same characteristics of the BCPs suggest that the electronic density topology of the hydrogen bond or the halogen bond is insensitive to the cooperative effects. This phenomenon is consistent with the results of the previous study of the isoguanine trimer.[48]

NBO Analysis. For a better understanding of the noncovalent bonds and their cooperativity, NBO analysis has been carried out at the HF/aug-cc-pVTZ level of theory using MP2(full)/aug-cc-pVDZ geometry. Some significant donor−acceptor orbital interactions and their second-order perturbation stabilization energies, provided by NBO analysis, are collected in Table 4.

Let us first repeat that the formation of a hydrogen-bonded complex, either conventional hydrogen bond or the blue-shifting hydrogen bond, involves charge transfer from the proton acceptor to the proton donor. This results in the increase of electron density in the X−H antibonding orbitals of the proton donor. For the halogen bond, the case is a little similar.[23] The charge transfer from the lone pairs of the electron donor in the halogen atom acceptor is mainly directed to the X−Br antibonding orbitals of the halogen atom donor, too. Since the charge-transfer accompanies the formation of hydrogen bonds or halogen bonds and plays a major role in it, ΔE^2 can be taken as an index to judge the strength of hydrogen bonds or halogen bonds. As can be seen from Table 4, the largest charge-transfer stabilization energies are computed to be 10.46, 5.63, 2.73, and 1.26 kcal/mol for n(O)−σ*(O−H), n(Br)−σ*(O−H), n(O)−σ*(C−H), and n(O)−σ*(C−Br) interactions, respectively, which are comparable in magnitude to their interaction energies. In comparing the stabilization energy terms in Table 4 with the corresponding density terms in Table 3, it is found that they correlate very well.

TABLE 4: Some Significant Donor−Acceptor Orbital Interactions and Their Second-Order Perturbation Stabilization Energies (ΔE^2, kcal/mol)[a]

structures	donor	acceptor	interaction	ΔE^2
M1	LP(1) Br	BD*(1) O_1-H_1	$n-\sigma^*$	0.17 (**0.18**)
	LP(3) Br	BD*(1) O_1-H_1	$n-\sigma^*$	5.63 (**5.02**)
	LP(1) O_1	BD*(1) O_2-H_2	$n-\sigma^*$	0.13 (**0.11**)
	LP(2) O_1	BD*(1) O_2-H_2	$n-\sigma^*$	10.46 (**9.79**)
	LP(1) O_2	BD*(1) C−H_3	$n-\sigma^*$	0.12 (**0.07**)
	LP(2) O_2	BD*(1) C−H_3	$n-\sigma^*$	2.73 (**2.47**)
M2	LP(1) Br	BD*(1) O_1-H_1	$n-\sigma^*$	0.19 (**0.18**)
	LP(3) Br	BD*(1) O_1-H_1	$n-\sigma^*$	4.04 (**3.59**)
	LP(1) O_1	BD*(1) O_2-H_2	$n-\sigma^*$	0.09 (**0.08**)
	LP(2) O_1	BD*(1) O_2-H_2	$n-\sigma^*$	7.03 (**6.84**)
	LP(1) O_2	BD*(1) C−Br	$n-\sigma^*$	0.12 (**0.11**)
	LP(2) O_2	BD*(1) C−Br	$n-\sigma^*$	1.26 (**1.16**)
M3	LP(3) Br	BD*(1) O_1-H_1	$n-\sigma^*$	1.57 (**1.63**)
	LP(1) O_1	BD*(1) C−H_3	$n-\sigma^*$	0.47 (**0.00**)
	LP(2) O_1	BD*(1) C−H_3	$n-\sigma^*$	0.58 (**0.81**)
	LP(1) O_2	BD*(1) O_1-H_2	$n-\sigma^*$	0.08 (**0.08**)
	LP(2) O_2	BD*(1) O_1-H_2	$n-\sigma^*$	7.56 (**7.55**)
M4	LP(2) Br	BD*(1) O_1-H_1	$n-\sigma^*$	0.50 (**0.00**)
	LP(3) Br	BD*(1) O_1-H_1	$n-\sigma^*$	1.85 (**2.43**)
	LP(2) Br	BD*(1) O_1-H_2	$n-\sigma^*$	0.69 (**0.00**)
	LP(3) Br	BD*(1) O_1-H_2	$n-\sigma^*$	1.62 (**2.38**)
	LP(1) O_1	BD*(1) C−H_3	$n-\sigma^*$	0.47 (**0.46**)
	LP(1) O_2	BD*(1) C−H_4	$n-\sigma^*$	0.33 (**0.33**)
	LP(2) O_2	BD*(1) C−H_4	$n-\sigma^*$	0.23 (**0.22**)

[a] Numbers in bold are values of the corresponding dimers. BD* denotes the formally empty antibonding orbital. LP denotes the occupied lone pair. All values are obtained at the HF/aug-cc-pVTZ level of theory.

On the other hand, the charge-transfer stabilization energies of structures **M1** and **M2** exhibit clear alteration compared to those of the related dimers. The charge-transfer stabilization energy values of **M1** and **M2** are generally larger than those in the related dimers (see Table 4). The increase is especially obvious for the n(O)−σ*(O−H) interaction. Large changes can also be seen for other interactions in structures **M1** and **M2**. A cooperative effect seems largely to influence the charge-transfer stabilization energy. For structures **M3** and **M4**, the charge transfer stabilization energies show very little change because there is no cooperativity in these trimers. Finally, we can conclude that, unlike the electronic density topology of the hydrogen bond or the halogen bond, the charge transfer stabilization energy is sensitive to the cooperative effect. This indicates the inductive effects to be mainly responsible for the trimer nonadditive effect.

Conclusions

In summary, we have systematically described the results of a quantum chemical study of the stability, structure, hydrogen bonding or halogen bonding pattern, topological analysis of the electronic density, and charge-transfer analysis of different orbitals of bromomethane−water 1:2 complexes. We conclude with the following remarks as answers to the questions put forth in the beginning:

(i) The bromine atom acts mainly as a proton acceptor in the four studied structures. It is also capable of participating in the formation of the halogen bond; for example, the bromine atom in **M2** acts as an electron acceptor in the halogen bond and an electron donor in the hydrogen bond and plays a dual role.

(ii) The most stable structure, **M1**, is cyclic with three different hydrogen bonds. The strongest cooperativity is observed for structure **M1**, where it amounts to 12% of the total binding energy. The cooperativity decreases in **M2** and becomes zero in **M3**. It is worth mentioning that the cooperativity in **M2** is derived from two hydrogen bonds and one halogen bond. A slightly destabilizing effect (anticooperativity) takes place in structure **M4** when the bromine atom acts as a double acceptor.

(iii) The changes of electron density and Laplacian at the bond critical point of the hydrogen bond or the halogen bond are insensitive to the cooperative effects.

(iv) The charge-transfer stabilization energy is sensitive to the cooperative effect, which indicates the donor−acceptor electron density transfer to be mainly responsible for the trimer nonadditive effect.

Acknowledgment. This work was supported by the Special Research Foundation of Doctoral Education of the Chinese University (Grant 20020610024), National Science Foundation of China (Grant 20373045), and Science Foundation of Huazhong University of Science and Technology.

Supporting Information Available: Optimized structure and Cartesian coordinates for the $CH_3Br\cdots H_2O$ complex, infrared spectra and Cartesian coordinates of four low-energy structures **M1**, **M2**, **M3**, and **M4**. This material is available free of charge via the Internet at http://pubs.acs.org.

References and Notes

(1) Lehn, J. M. *Supramolecular Chemistry*: *Concepts and Perspectives*; VCH: Weinheim, Germany, 1995.

(2) Desiraju, G. R. *Crystal Engineering*: *The Design of Organic Solids*; Elsevier: Amsterdam, The Netherlands, 1989.

(3) Desiraju, G. R.; Steiner, T. *The Weak Hydrogen Bond In Structural Chemistry and Biology*; Oxford University Press: New York, 1997.

(4) Nishio, M.; Hirota, M.; Umezawa, Y. *The CH−Interaction*; Wiley-VCH: New York, 1998.

(5) Scheiner, S., Ed. *Molecular Interactions*: *From van der Waals to Strong Bound Complexes*; Wiley: Chichester, UK, 1997.

(6) Jeffrey, J. A.; Saenger, W. *Hydrogen Bonding in Biological Structures*; Springer-Verlag: Berlin, Germany, 1991.

(7) Umeyama, H.; Morokuma, K.; Yamabe, S. *J. Am. Chem. Soc.* **1977**, *99*, 330.

(8) Kollman, P.; Dearling, A.; Kochanski, E. *J. Phys. Chem.* **1982**, *86*, 1607.

(9) Røeggen, I.; Dahl, T. *J. Am. Chem. Soc.* **1992**, *114*, 511.

(10) (a) Price, S. L.; Stone, A. J.; Lucas, J.; Rowland, R. S.; Thornley, A. E. *J. Am. Chem. Soc.* **1994**, *116*, 4910. (b) Lommerse, J. P. M.; Stone, A. J.; Taylor, R.; Allen, F. H. *J. Am. Chem. Soc.* **1996**, *118*, 3108.

(11) (a) Legon, A. C.; Lister, D. G.; Thorn, J. C. *J. Chem. Soc., Chem. Commun.* **1994**, 757. (b) Legon, A. C.; Lister, D. G.; Thorn, J. C. *J. Chem. Soc., Faraday Trans.* **1994**, *90*, 3205. (c) Bloemink, H. I.; Legon, A. C.; Thorn, J. C. *J. Chem. Soc., Faraday Trans.* **1994**, *90*, 781. (d) Legon, A. C. *J. Chem. Soc., Faraday Trans.* **1995**, *91*, 781. (e) Legon, A. C. *Chem. Eur. J.* **1998**, *4*, 1890.

(12) Desiraju, G. R. *Angew. Chem., Int. Ed. Engl.* **1995**, *34*, 2311.

(13) Latajka, Z.; Berski, S. *J. Mol. Struct.* (*THEOCHEM*) **1996**, *371*, 11.

(14) Ruiz, E.; Salahub, D. R.; Vela, A. *J. Phys. Chem.* **1996**, *100*, 12265.

(15) Bosch, E.; Barnes, C. L. *Cryst. Growth Des.* **2002**, *2*, 299.

(16) Bürger, H. *Angew. Chem., Int. Ed. Engl.* **1997**, *36*, 718.

(17) Zhang, Y.; Zhao, C.-Y.; You, X.-Z. *J. Phys. Chem. A* **1997**, *101*, 2879.

(18) Alkorta, I.; Rozas, I.; Elguero, J. *J. Phys. Chem. A* **1998**, *102*, 9278.

(19) Amico, V.; Meille, S. V.; Corradi, E.; Messina, M. T.; Resnati, G. *J. Am. Chem. Soc.* **1998**, *120*, 8261.

(20) Farina, A.; Meille, S. V.; Messina, M. T.; Metrangolo, P.; Resnati, G.; Vecchio, G. *Angew. Chem., Int. Ed.* **1999**, *38*, 2433.

(21) Corradi, E.; Meille, S. V.; Messina, M. T.; Metrangolo, P.; Resnati, G. *Angew. Chem., Int. Ed.* **2000**, *39*, 1782.

(22) Valerio, G.; Raos, G.; Meille, S. V.; Metrangolo, P.; Resnati, G. *J. Phys. Chem. A* **2000**, *104*, 1617.

(23) Karpfen, A. *J. Phys. Chem. A* **2000**, *104*, 6871.

(24) Walsh, R. B.; Clifford W.; Padgett, C. W.; Metrangolo, P.; Resnati, G.; Hanks, T. W.; Pennington, W. T. *Cryst. Growth Des.* **2001**, *1*, 165.

(25) (a) Metrangolo, P.; Resnati, G. *Chem. Eur. J.* **2001**, *7*, 2511. (b) Metrangolo, P.; Neukirch, H.; Pilati, T.; Resnati, G. *Acc. Chem. Res.* **2005**, *38*, 386.

(26) Romaniello, P.; Lelj, F. *J. Phys. Chem. A* **2002**, *106*, 9114.

(27) Nangia, A. *CrystEngComm*. **2002**, *17*, 1.

(28) Burton, D. D.; Fontana, F.; Metrangolo, P.; Pilatid T.; Resnatic, G. *Tetrahedron Lett.* **2003**, *44*, 645.

(29) Wang, W.; Wong, N.; Zheng, W.; Tian, A. *J. Phys. Chem. A* **2004**, *108*, 1799.

(30) Zou, J. W.; Jiang, Y. J.; Guo, M.; Hu, G. X.; Zhang, B.; Liu, H. C.; Yu, Q. S. *Chem. Eur. J.* **2005**, *11*, 740.

(31) (a) Hays, F. A.; Vargason, J. M.; Ho, P. S. *Biochemistry* **2003**, *42*, 9586. (b) Auffinger, P.; Hays, F. A.; Westhof, E.; Ho, P. S. *Proc. Natl. Acad. Sci. U.S.A.* **2004**, *101*, 16789.

(32) (a) Zhu, S. F.; Zhu, S. Z.; Liao, Y. X.; Huang, C. F.; Li, Z. T. *Chin. J. Chem.* **2004**, *22*, 896. (b) Zhu, S. Z.; Xing, C. H.; Xu, W.; Jin, G. F.; Li, Z. T. *Cryst. Growth Des.* **2001**, *4*, 53.

(33) There is only one minimum, which has cyclic double hydrogen-bonded geometry, on the MP2(full)/aug-cc-pVDZ $CH_3Br\cdots H_2O$ potential energy surface (see the Supporting Information). The halogen-bonded geometry of the $CH_3Br\cdots H_2O$ complex is not a minimum but rather a second-order stationary point on the surface. The halogen bond is also hard to form in other $CH_3Br(H_2O)_n$ ($n > 2$) complexes due to the very strong tendency to transform into a stronger $O-H\cdots O$ hydrogen bond.

(34) Møller, C.; Plesset, M. S. *Phys. Rev.* **1934**, *46*, 618.

(35) Hobza, P.; Šponer, J. *Chem. Rev.* **1999**, *99*, 3247.

(36) Krishnan, R.; Binkley, J. S.; Seeger, R.; Pople, J. A. *J. Chem. Phys.* **1980**, *72*, 650.

(37) (a) Boyd, R. J.; Choi, S. C. *Chem. Phys. Lett.* **1985**, *120*, 80. (b) Boyd, R. J.; Choi, S. C. *Chem. Phys. Lett.* **1986**, *129*, 62. (c) Carroll, M. T.; Chang, C.; Bader, R. F. W. *Mol. Phys.* **1988**, *63*, 387. (d) Carroll, M. T.; Bader, R. F. W. *Mol. Phys.* **1988**, *65*, 695.

(38) (a) Dunning, T. H., Jr. *J. Chem. Phys.* **1989**, *90*, 1007. (b) Woon, D. E.; Dunning, T. H., Jr. *J. Chem. Phys.* **1993**, *98*, 1358. It is well known that the aug-cc-pVXZ series of basis sets was designed for frozen-core MP2 calculations. Here, we employed the aug-cc-pVDZ and aug-cc-pVTZ basis sets for fully correlated calculations because our test calculations clearly showed that the values of the counterpoise-corrected binding energies obtained using fully correlated MP2 calculations are more close to their CBS limit values than those obtained using frozen-core MP2 calculations.

(39) Boys, S. F.; Bernardi, F. *Mol. Phys.* **1970**, *19*, 553.

(40) Bader, R. F. W. *Atoms in Molecules*: *A Quantum Theory*; Clarendon; Oxford, U.K., 1990.

(41) (a) Reed, A. E.; Weinstock, R. B.; Weinhold, F. *J. Chem. Phys.* **1985**, *83*, 735. (b) Reed, A. E.; Weinstock, R. B.; Weinhold, F. *J. Chem. Phys.* **1985**, *83*, 1736. (c) Reed, A. E.; Curitss, L. A.; Weinhold, F. *Chem. Rev.* **1988**, *88*, 889.

(42) Frisch, M. J.; Trucks, G. W.; Schlegel, H. B.; Scuseria, G. E.; Robb, M. A.; Cheeseman, J. R.; Montgomery, J. A., Jr.; Vreven, T.; Kudin, K. N.; Burant, J. C.; Millam, J. M.; Iyengar, S. S.; Tomasi, J.; Barone, V.; Mennucci, B.; Cossi, M.; Scalmani, G.; Rega, N.; Petersson, G. A.; Nakatsuji, H.; Hada, M.; Ehara, M.; Toyota, K.; Fukuda, R.; Hasegawa, J.; Ishida, M.; Nakajima, T.; Honda, Y.; Kitao, O.; Nakai, H.; Klene, M.; Li, X.; Knox, J. E.; Hratchian, H. P.; Cross, J. B.; Adamo, C.; Jaramillo, J.; Gomperts, R.; Stratmann, R. E.; Yazyev, O.; Austin, A. J.; Cammi, R.; Pomelli, C.; Ochterski, J. W.; Ayala, P. Y.; Morokuma, K.; Voth, G. A.; Salvador, P.; Dannenberg, J. J.; Zakrzewski, V. G.; Dapprich, S.; Daniels, A. D.; Strain, M. C.; Farkas, O.; Malick, D. K.; Rabuck, A. D.; Raghavachari, K.; Foresman, J. B.; Ortiz, J. V.; Cui, Q.; Baboul, A. G.; Clifford, S.; Cioslowski, J.; Stefanov, B. B.; Liu, G.; Liashenko, A.; Piskorz, P.; Komaromi, I.; Martin, R. L.; Fox, D. J.; Keith, T.; Al-Laham, M. A.; Peng, C. Y.; Nanayakkara, A.; Challacombe, M.; Gill, P. M. W.; Johnson,

B.; Chen, W.; Wong, M. W.; Gonzalez, C.; Pople, J. A. *Gaussian 03*, Revision C.02; Gaussian, Inc.: Wallingford CT, 2004.

(43) Biegler-König F.; Schönbohm, J.; Bayles, D. *J. Comput. Chem.* **2001**, *22*, 545.

(44) (a) Gu, Y.; Kar, T.; Scheiner, S. *J. Am. Chem. Soc.* **1999**, *121*, 9411. (b) Hobza, P.; Havlas, Z. *Chem. Rev.* **2000**, *100*, 4253. (c) Li, X.; Liu, L.; Schlegel, H. B. *J. Am. Chem. Soc.* **2002**, *124*, 9639. (d) Alabugin, I. V.; Manoharan, M.; Peabody, S.; Weinhold, F. *J. Am. Chem. Soc.* **2003**, *125*, 5973.

(45) Hobza, P.; Špirko, V.; Selzle, H. L.; Schlag, E. W. *J. Phys. Chem. A* **1998**, *102*, 2501.

(46) Koch, U.; Popelier, P. L. A. *J. Phys. Chem.* **1995**, *99*, 9747.

(47) Popelier, P. L. A. *J. Phys. Chem. A* **1998**, *102*, 1873.

(48) Gu, J.; Wang, J.; Leszczynski, J. *J. Phys. Chem. B* **2004**, *108*, 8017.